Published in final edited form as:
*J Magn Reson*. 2007 February ; 184(2): 228–235.

# Sensitivity and Resolution Enhancement in Solid-State NMR Spectroscopy of Bicelles

**Sergey V. Dvinskikh**[1], **Kazutoshi Yamamoto**, **Ulrich H. N. Dürr**, and **Ayyalusamy Ramamoorthy**[*]
*Biophysics Research Division and Department of Chemistry, The University of Michigan, Ann Arbor, MI 48109-1055, USA*

## Abstract

Magnetically aligned bicelles are becoming attractive model membranes to investigate the structure, dynamics, geometry, and interaction of membrane-associated peptides and proteins using solution- and solid-state NMR experiments. Recent studies have shown that bicelles are more suitable than mechanically aligned bilayers for multidimensional solid-state NMR experiments. In this work, we describe experimental aspects of the natural abundance $^{13}C$ and $^{14}N$ NMR spectroscopy of DMPC/DHPC bicelles. In particular, approaches to enhance the sensitivity and resolution and to quantify radio frequency heating effects are presented. Sensitivity of $^{13}C$ detection using single pulse excitation, conventional cross-polarization (CP), ramp-CP, and NOE techniques are compared. Our results suggest that the proton decoupling efficiency of the FLOPSY pulse sequence is better than that of continuous wave decoupling, TPPM, SPINAL and WALTZ sequences. A simple method of monitoring the water proton chemical shift is demonstrated for the measurement of sample temperature and calibration of the radio-frequency-induced heating in the sample. The possibility of using $^{14}N$ experiments on bicelles is also discussed.

### Keywords

Bicelles; Sensitivity; Resolution; RF Heating; Proton Decoupling; Nitrogen-14 NMR

## 1. Introduction

The molecular aggregates formed by phospholipids in aqueous solution, which usually exist as bilayers in the form of vesicles, gels, or lamellae, are often used as models for cell membranes. Although the disordered multilamellar vesicles have extensively been used in NMR studies, the macroscopically oriented phases have the advantage of preserving anisotropic spin interactions that offer a wealth of information about the molecular geometry and dynamics [1]. Therefore, considerable efforts have been devoted to develop magnetically oriented phospholipid bilayers [2–9]. While several studies have reported on the preparation, characterization and applications of bicelles [4–6,8], a systematic optimization of solid-state NMR experiments on bicelles is lacking.

*Corresponding author email: ramamoor@umich.edu Tel. # 734-647-6572.
[1]Present address: Division of Physical Chemistry, Department of Chemistry, Royal Institute of Technology, Stockholm, Sweden

Since molecules embedded in bicelles are dynamic, the molecular motion could degrade the efficiency of solid-state NMR pulse sequences. For example, it is difficult to establish an experimental condition that efficiently transfers magnetization from protons to carbons (or other low sensitive nuclei) at all sites of a molecule, and also for all molecules, in a bicelle sample. A short contact time cross-polarization (CP) [10] sequence is more efficient for rigid parts of a molecule than for mobile regions, as heteronuclear dipolar couplings in the latter case are averaged by the motion [11,12]. On the other hand, a long contact time or the NOE (nuclear Overhauser effect)-type magnetization transfer may be better for mobile sites of a molecule [13]. In this study, we have compared the efficiencies of different methods to enhance the sensitivity of $^{13}C$ signal from bicelles.

The use of high RF (radio frequency) decoupling field strengths is necessary to achieve line-narrowing in most solid-state NMR applications [14,15]. Proton decoupling in the form of multiple pulse sequences is commonly used to record signals of less sensitive nuclei (such as $^{13}C$ and $^{15}N$). An actual RF power required to accomplish an efficient proton decoupling depends on the design of a decoupling pulse sequence. The use of high RF field strengths, which becomes important for experiments at high magnetic fields, however, generates sample heating because of the RF power dissipation within the sample. A majority of biological samples are very susceptible to RF-induced heating, because of the interaction of fast oscillating fields with ions in salty samples and/or the electric dipolar moment of the molecules in dielectrics [16–19]. These effects are a major concern in the application of multidimensional SLF (separated-local-field) [20,21] experiments to static samples such as bicelles. Since most physicochemical properties of biological molecules depend on the sample temperature, an adequate temperature control during NMR experiments is, therefore, important. The RF heating effects are not typically measurable from the readings of a variable-temperature control unit of an NMR spectrometer, and therefore they must be properly calibrated and corrected prior to an experiment. In this study, we propose a simple method to measure the sample temperature during solid-state NMR experiments on bicelles. The efficiency of various proton decoupling sequences and the requirement of the RF field strength are also analyzed in this study.

## 2. Results and Discussion

### 2.1. Sample heating due to an RF irradiation

To assess the sample heating induced by the $^{1}H$ decoupling, we used the high sensitivity of the water proton chemical shift to the sample temperature [22,23]. Figure 1(a) shows the temperature dependence of the water proton chemical shift. The slope is 0.010 ± 0.001 ppm/°C (or 4.0 ± 0.4 Hz/°C at a magnetic field of 9.4 T), which is similar to the value reported for the pure water [22]. The experimental setup used in this study resulted in a line width of 23 Hz, thus providing an accuracy of about 0.6°C in the sample temperature measurement. To measure the RF-induced sample heating, an RF irradiation emulating the heteronuclear decoupling sequence was applied at the proton resonance frequency and, after a short magnetization recovery period, the proton FID signal was recorded following a 90° pulse. A 40 ms RF irradiation time corresponding to the $^{1}H$ decoupling time in $^{13}C$ experiments was used. A delay of 200 ms after the decoupling pulse required for the magnetization recovery was chosen sufficiently short to avoid significant heat dissipation in the sample before acquiring the spectrum. For each measurement, 16 transients with a delay of 5 seconds were accumulated preceded by 16 dummy scans to ensure a steady state sample temperature. The heating effect in the bicelle sample versus the RF field strength is presented in Figure 1(b). In agreement with theory [24,25], a second power dependence of the heating effect on the RF power was observed. The temperature gradient in the sample volume induced by the RF irradiation was estimated from the increase in the linewidth of the $^{1}H_2O$ peak. The results are

also included in Figure 1(b). In principle, the average temperature shift can be corrected by adjusting the setting on the temperature control unit. On the other hand, the temperature gradient within the sample and the heating during the decoupling pulse cannot be dealt with in that way.

In the $^{13}C$ experiments presented below, a 20 kHz proton-decoupling field was typically used. This resulted in an increase of the average sample temperature by about 2°C. A comparable effect is also expected due to the RF irradiation of protons during the indirect period ($t_1$) of a 2D experiment. For example, the popular PISEMA (polarization inversion spin exchange at the magic angle) experiment [13,26–28] and other rotating-frame SLF experiments [29–35] for the measurement of the heteronuclear dipolar coupling utilize a high RF power in the $t_1$ period. On the other hand, the effect of the RF irradiation on the $^{13}C$ channel (for example, as applied in a cross-polarization sequence, and also during the evolution period of rotating-frame experiments) was found to be negligible. This stems from less power losses at a lower RF frequency [24]. Generally, experiments at a higher magnetic field lead to more significant sample heating due to a higher resonance frequency [24] and also due to wider signal dispersion by the chemical shift which requires a stronger RF field for effective decoupling of protons. The amount of heating may also depend on the sample size and geometry [36,37], sample composition [17,19,38], RF coil design [37,39,40], and the flow-rate of the heating/cooling gas [24]. Therefore, the calibration of the RF heating effect on each sample is required for an experimental set-up. Finally, we note that the recent developments in the probe and coil design minimizing the electric field inside the sample provide a significant reduction of sample heating [40].

## 2.2. Signal enhancement

In NMR spectroscopy of low-gamma nuclei in liquids, the common approaches for sensitivity enhancement are *J*-coupling mediated polarization transfer using the INEPT (*i*nsensitive *n*uclei *e*nhanced by *p*olarization *t*ransfer) sequence [41] and heteronuclear cross-relaxation under the condition of saturating $^{1}H$ RF field using NOE [42]. In solids, on the other hand, CP in the rotating frame [10] is the most popular technique, which is also frequently used in anisotropic biological samples. However, the motional averaging in bicelles reduces C-H dipolar couplings, as compared to rigid solids, and results in an increased sensitivity to the Hartmann-Hahn mismatch [43] of RF fields during CP. Hence, a ramp-CP sequence [44] is advantageous to overcome the Hartmann-Hahn mismatch [10,43]. On the other hand, high molecular mobility may favour the NOE approach [45], which becomes efficient when the correlation time of the motion is small compared to the inverse of resonance frequency. The INEPT transfer is not practical in static anisotropic samples, since the $J_{CH}$ couplings are unresolved in the presence of strong residual heteronuclear dipolar interactions. (INEPT, however, has been employed in lipid bilayer samples under the MAS condition, when dipolar couplings are suppressed by the sample spinning [45].)

In Figure 2, $^{13}C$ chemical shift spectra obtained by single pulse excitation (SPE), conventional CP [10], ramp-CP [44], and NOE [45] techniques are compared. Overall, the ramp-CP [44] provides the largest enhancement factor (of about 3 with respect to SPE) in our sample for most of the sites. The optimal contact time in CP strongly differs for various sites in the molecule resulting in a non-uniform enhancement. NOE is superior only for the most mobile groups, the γ and $C_{14}$ sites of a lipid molecule.

## 2.3. Heteronuclear decoupling

Since RF heating is a problem for NMR studies on bicelles, it is important to effectively utilize the RF power of pulse sequences. A long data acquisition under proton decoupling, needed to obtain a high-resolution $^{13}C$ chemical shift spectrum of bicelles, is an obvious heat-generating

part of an experiment and therefore needs to be optimized. It is known that the RF power needed to achieve efficient heteronuclear spin decoupling depends on the design of a decoupling sequence [46]. A careful choice of the decoupling scheme is, therefore, important to obtain highly resolved $^{13}C$ spectra at a limited RF power level. We examined the performances of decoupling sequences that are frequently used in studies on biological samples and liquid crystals. In particular, we investigated the efficiencies of TPPM (two pulse phase-modulation) [47], SPINAL-64 (small phase incremental alternation) [48], WALTZ-16 (wideband alternating phase low-power technique for zero residue splitting) [49] and FLOPSY-8 (flip flop spectroscopy) [50] schemes, and compared them to a conventional continuous wave (CW) decoupling. The $^{13}C$ chemical shift spectra acquired using different decoupling schemes are presented in Figure 3. The $^{1}H$ RF field strength was 20 kHz and the decoupler frequency was set to obtain the best resolution in the most crowded $^{13}C$ spectral region, 30–36 ppm, by applying a CW irradiation. For the acyl chain $^{13}C$ signals, the performances of TPPM, SPINAL-64, and FLOPSY-8 decoupling sequences are comparable and significantly better than CW and WALTZ sequences. Excellent resolution was achieved using the FLOPSY-8 pulse sequence scheme, which was originally designed for the broadband homonuclear cross-polarization in liquids [50], but was also used for heteronuclear decoupling in lyotropic liquid crystalline systems [51]. Compared to the SPINAL-64 decoupling, use of the FLOPSY-8 sequence improved the spectral resolution for the head group and glycerol carbons; in particular for $g_2$, $g_3$, and β sites (Fig. 3). In addition the FLOPSY sequence is relatively easy to set up since it requires only adjusting the single parameter, the 180° pulse length, and is very tolerant to the miscalibration of the pulse length.

Figure 4 compares the $^{13}C$ chemical shift spectra of a bicellar sample obtained at different RF power levels using the FLOPSY-8 decoupling. Notably, an RF field strength as low as 16 kHz is sufficient to achieve adequate resolution comparable to that obtained using other sequences at much higher fields. It is interesting to note that very strong decoupling fields, up to 80 kHz, were commonly employed in similar systems [45]. It should be pointed out that a previous study on magnetically aligned bicelles containing a peptide suggested that a SPINAL-16 [48] decoupling sequence provided a better decoupling performance than other decoupling sequences analyzed [52]; however, the performance of the FLOPSY sequence was not examined in that study. Our results suggest that broadband sequences like FLOPSY can provide significant advantage in bicellar systems.

### 2.4. Nitrogen-14 NMR spectra of bicelles

The electric field gradient around the $^{14}N$ nucleus, and hence the quadrupole coupling, is considerably reduced due to the near-tetrahedral symmetry of the choline groups of DMPC and DHPC molecules [53–57]. The dynamics of the lipid head group further reduces the quadrupole coupling to about 20 kHz. Therefore, the detection of $^{14}N$ in bicelles requires neither extremely short pulses nor a wide spectral window.

Nitrogen-14 spectra of aligned bicelles are given in Figure 5. Two sets of narrow doublet peaks are observed in the spectra. The doublet with a larger quadrupole splitting arises from DMPC as it is similar to the spectra obtained from mechanically aligned DMPC or POPC bilayers [54], while the doublet with a smaller splitting corresponds to the DHPC molecule. *Flipped bicelle*s [58] are characterized by the orientation of the bilayer normal along the external magnetic field. As demonstrated in Figure 5(B), in a *flipped bicelle* sample the quadrupolar splittings are nearly doubled compared to that of unflipped bicelles in correspondence with the direction of the alignment.

As seen from spectra of bicelles containing ligands, $^{14}N$ is very sensitive to the ligand-lipid interactions that alter the electric field gradient surrounding the $^{14}N$ nucleus. For example, the presence of an amphipathic, α-helical antimicrobial peptide, MSI-78 [59], significantly reduces

the quadrupole splitting of DMPC (Figures 5 D & E). Since MSI-78 is cationic with a net charge of +9 and interacts with the lipid headgroups, it could interfere with the cross-linking of lipids. This would enhance the symmetry of the positively charged choline group and therefore reduce the quadrupole splitting. Similar effects have been utilized in probing the interaction of antidepressants with membranes in mechanically aligned bilayers. A sample spectrum of bicelles containing an antidepressant, desipramine, is given in Figure 5(C), which shows the expected reduction in the $^{14}$N quadrupole splitting [54]. Interestingly, the presence of an anionic lipid, DMPG, slightly increases the quadrupole coupling of DMPC as well as DHPC while the line width depends on the concentration of salt in the sample (Figures 5 F & G). While more experimental analyses are needed to understand the observed changes in the $^{14}$N quadrupole coupling, these results suggest that $^{14}$N NMR spectroscopy of magnetically aligned bicelles can be used as a 'voltmeter' to measure the interaction of ligands with membranes. It should be mentioned here that the measurement of the $^{14}$N quadrupole coupling of the choline group was recently utilized to understand the membrane-interaction of charged molecules such as antimicrobial peptides in mechanically aligned bilayers and also in multilamellar vesicles under static and MAS conditions [60–62].

## 3. Conclusions

In this study, we investigated various practical aspects of $^{13}$C and $^{14}$N NMR experiments in magnetically oriented bicelles. We have demonstrated that RF heating effects in bicellar samples can easily be calibrated and taken into account by monitoring the water proton chemical shift. This approach can be used for studies on other samples like mechanically aligned bilayers and multilamellar vesicles as well. We have also demonstrated that by applying advanced broadband decoupling sequences the required decoupling RF power can be considerably reduced and thus RF heating can be minimized. A comparison of various methods to enhance the sensitivity of experiments to detect less sensitive nuclei and to enhance the resolution of the chemical shift spectrum of less sensitive nuclei in bicelles is presented. Our results infer that $^{14}$N NMR experiments on bicelles are easy to carry out with a standard commercial set-up. The detection of $^{14}$N nuclei could be used as a 'voltmeter' to study ligand-membrane interactions. We believe that the results presented in this paper can be utilized in performing advanced multidimensional solid-state NMR experiments [63–65] on bicelles containing peptides, proteins, drugs or other types of molecules.

## 4. Experimental Section

### 4.1. Sample preparation

1,2-dimyristoyl-*sn*-glycero-3-phosphatidylcholine (DMPC) and 1,2-dihexanoyl-*sn*-glycero-3-phosphatidylcholine (DHPC) were purchased from Avanti Polar Lipids, Inc. (Alabaster, AL). DMPC and DHPC with a molar ratio (*q*=DMPC:DHPC) of 3.5:1 was dissolved in chloroform. The solvent was slowly evaporated under a stream of nitrogen gas at room temperature and completely removed by overnight lyophilization. A 100 mM HEPES buffer at pH 7.0 was added to obtain a concentration of 37.5% (w/w) phospholipids to solution. Peptide was cosolubilized in chloroform along with the lipids at the desired molar ratios, while an appropriate amount of $YbCl_3$ salt was added to the HEPES buffer to yield 'flipped' bicelles [66,67]. The sample was vortexed until all of the lipids were solubilized in the HEPES buffer. The solubilized sample was gently sonicated in an ice-cold water bath. The final sample was obtained by several freeze and thaw cycles until a clear transparent solution was formed.

### 4.2. NMR measurements

All NMR experiments were carried out on a Chemagnetics/Varian Infinity-400 MHz solid-state NMR spectrometer using a 5 mm custom-modified double-resonance magic-angle

spinning probe under static sample conditions. About 100 mg of sample was loaded in a 5 mm NMR glass tube of 4 cm length and was closed tightly with a Teflon tape and a cap. The sample was equilibrated prior to the measurement for about 1 hour in the magnet at 37°C. All experiments were performed at 37°C. Phosporus-31 chemical shift spectra were recorded to test the magnetic alignment of bicelles. A ramped-CP [44] sequence with a contact time of 5 ms was used to record the 1D $^{13}$C chemical shift spectra under proton decoupling using various decoupling sequences for a comparative study. A 5 μs $^{1}$H 90° pulse, a recycling delay of 7 s, a 25 kHz spectral width, and an acquisition time of 41 ms were used. Data were processed without any line broadening. For the NOE enhancement, protons were irradiated using a 1 kHz RF field during the recycling delay.

To record signals of $^{14}$N NMR spectra the quadrupole echo sequence (68) was used with the pulse length of 4.4 μs and an echo-delay of 1 ms. With this long delay the interference effect of the probe acoustic ringing, which is severe at the $^{14}$N resonance frequency of 29 MHz, was negligible. No influence of the proton decoupling on the $^{14}$N spectral shape was observed. Hence, spectra presented here were acquired without the proton decoupling. Up to 4,000 scans were accumulated with a repetition delay of 0.2 s.

**Acknowledgements**

We would like to thank Prof. Gary Lorigan and his research group at the Miami University for their help with the preparation of bicelles. This study was supported by the research funds from National Institutes of Health (AI054515).

## References

1. Opella SJ, Marassi FM. Structure determination of membrane proteins by NMR spectroscopy. Chem Rev 2004;104:3587–3606. [PubMed: 15303829]
2. Prosser RS, Evanics F, Kitevski JL, Al-Abdul-Wahid MS. Current applications of bicelles in NMR studies of membrane-associated amphiphiles and proteins. Biochemistry 2006;45:8453–8465. [PubMed: 16834319]
3. Sanders CR, Prosser RS. Bicelles: a model membrane system for all seasons? Structure 1998;6:1227–1234. [PubMed: 9782059]
4. Sanders CR, Prestegard JH. Magnetically orientable phospholipid bilayers containing small amounts of a bile salt analogue, CHAPSO. Biophys J 1990;58:447–460. [PubMed: 2207249]
5. Sanders CR, Schwonek JP. Characterization of magnetically orientable bilayers in mixtures of dihexanoylphosphatidylcholine and dimyristoylphosphatidylcholine by solid-state NMR. Biochemistry 1992;31:8898–8905. [PubMed: 1390677]
6. Sanders CR, Hare BJ, Howard KP, Prestegard JH. Magnetically-oriented phospholipid micelles as a tool for the study of membrane-associated molecules. Prog Nucl Magn Reson Spectrosc 1994;26:421–444.
7. Nevzorov, AA.; DeAngelis, AA.; Park, SH.; Opella, SJ. Uniaxial motional averaging of the chemical shift anisotropy of membrane proteins in bilayer environments; Chapter 7. In: Ramamoorthy, A., editor. NMR Spectroscopy of Biological Solids. Taylor & Francis; New York: 2005.
8. Lorigan, GA. Solid-state magnetic resonance spectroscopic studies of magnetically aligned phospholipids bilayers, Chapter 10. In: Ramamoorthy, A., editor. NMR Spectroscopy of Biological Solids. Taylor & Francis; New York: 2005.
9. Marcotte I, Auger M. Bicelles as model membranes for solid- and solution-state NMR studies of membrane peptides and proteins. Concep Magn Reson, Part A 2005;24:17–37.
10. Pines A, Gibby MG, Waugh JS. Proton-enhanced NMR of dilute spins in solids. J Chem Phys 1973;59:569–590.
11. Kim H, Cross TA, Fu RQ. Cross-polarization schemes for peptide samples oriented in hydrated phospholipid bilayers. J Magn Reson 2004;168:147–152. [PubMed: 15082260]
12. Lee DK, Santos JS, Ramamoorthy A. Application of one-dimensional dipolar-shift solid-state NMR spectroscopy to study the backbone conformation of membrane-associated peptides in phospholipid bilayers. J Phys Chem 1999;B103:8383.

13. Katoh E, Takegoshi K, Terao KT. C-13 nuclear Overhauser polarization-magic- angle spinning nuclear magnetic resonance spectroscopy in uniformly C-13-labeled solid proteins. J Am Chem Soc 2004;126:3653–3657. [PubMed: 15025494]
14. Haeberlen U, Waugh JS. Coherent Averaging Effects in Magnetic Resonance. Physical Review 1968;175:453.
15. Mehring, M. Principles of High Resolution NMR in Solids. 2. Springer-Verlag; Heidelberg: 1983.
16. Kelly AE, Ou HD, Withers R, Dotsch V. Low-conductivity buffers for high-sensitivity NMR measurements. J Am Chem Soc 2002;124:12013–12019. [PubMed: 12358548]
17. Li CG, Mo YM, Hu J, Chekmenev E, Tian CL, Gao FP, Fu RQ, Gor'kov P, Brey W, Cross TA. Analysis of RF heating and sample stability in aligned static solid-state NMR spectroscopy. J Magn Reson 2006;180:51–57. [PubMed: 16483809]
18. Lee DK, Wildman KAH, Ramamoorthy A. Solid-state NMR spectroscopy of aligned lipid bilayers at low temperatures. J Am Chem Soc 2004;126:2318–2319. [PubMed: 14982431]
19. Martin RW, Zilm KW. Variable temperature system using vortex tube cooling and fiber optic temperature measurement for low temperature magic angle spinning NMR. J Magn Reson 2004;168:202–209. [PubMed: 15140428]
20. Waugh JS. Uncoupling of local field spectra in nuclear magnetic resonance -determination of atomic positions in solids. Proc Natl Acad Sci USA 1976;73:1394–1397. [PubMed: 1064013]
21. Ramamoorthy A, Wei Y, Lee DK. PISEMA solid-state NMR spectroscopy. Annu Rep NMR Spectrosc 2004;52:1–52.
22. Hindman JC. Proton resonance shift of water in the gas and liquid states. J Chem Phys 1966;44:4582–4592.
23. Dvinskikh SV, Castro V, Sandström D. Heating caused by radiofrequency irradiation and sample rotation in $^{13}C$ magic angle spinning NMR studies of lipid membranes. Magn Reson Chem 2004;42:875–81. [PubMed: 15366061]
24. Led JJ, Petersen SB. Heating effects in carbon-13 NMR spectroscopy on aqueous solutions caused by proton noise decoupling at high frequencies. J Magn Reson 1978;32:1–17.
25. Kugel H. Improving the Signal-to-Noise Ratio of NMR Signals by Reduction of Inductive Losses. J Magn Reson 1991;91:179–l 85.
26. Wu CH, Ramamoorthy A, Opella SJ. High-resolution heteronuclear dipolar solid-state NMR spectroscopy. J Magn Reson A 1994;109:270–272.
27. Ramamoorthy A, Opella SJ. Two-dimensional chemical shift / heteronuclear dipolar coupling spectra obtained with polarization inversion spin exchange at the magic angle and magic-angle sample spinning (PISEMAMAS). Solid state NMR Spectrosc 1995;4:387.
28. Ramamoorthy A, Wu CH, Opella SJ. Experimental aspects of multidimensional solid-state NMR correlation spectroscopy. J Magn Reson 1999;140:131–140. [PubMed: 10479555]
29. Hester RK, Ackerman JL, Neff BL, Waugh JS. Separated local field spectra in NMR: Determination of structure in solids. Phys Rev Lett 1976;36:1081–1083.
30. Yamamoto K, Lee DK, Ramamoorthy A. Broadband-PISEMA solid-state NMR spectroscopy. Chem Phys Lett 2005;407:289–293.
31. Yamamoto K, Dvinskikh SV, Ramamoorthy A. Measurement of heteronuclear dipolar couplings using a rotating frame solid-state NMR experiment. Chem Phys Lett 2006;419:533–536.
32. Dvinskikh SV, Yamamoto K, Ramamoorthy A. Separated local field NMR spectroscopy by windowless isotropic mixing. Chem Phys Lett 2006;419:168–173.
33. Nevzorov AA, Opella SJ. A "Magic Sandwich" pulse sequence with reduced offset dependence for high-resolution separated local field spectroscopy. J Magn Reson 2003;164:182–186. [PubMed: 12932472]
34. Lee DK, Narasimhaswamy T, Ramamoorthy A. PITANSEMA A low-power PISEMA solid-state NMR experiment. Chem Phys Lett 2004;399:359–362. [PubMed: 16741561]
35. Dvinskikh SV, Yamamoto K, Ramamoorthy A. Heteronuclear isotropic mixing separated local field NMR spectroscopy. J Chem Phys 2006;125:034507.
36. Hoult DI, Lauterbur PC. The sensitivity of the zeugmatographic experiment involving human samples. J Magn Reson 1979;34:425–433.

37. Doty, FD. Encyclopedia of nuclear magnetic resonance. Grant, DM.; Harris, RK., editors. Wiley; Chichester: 1996. p. 3753
38. Marassi FM, Crowell KJ. Hydration-optimized oriented phospholipid bilayer samples for solid-state NMR structural studies of membrane proteins. J Magn Reson 2003;161:64–69. [PubMed: 12660112]
39. Stringer JA, Bronnimann CE, Mullen CG, Zhou DHH, Stellfox SA, Li Y, Williams EH, Rienstra CM. Reduction of RF-induced sample heating with a scroll coil resonator structure for solid-state NMR probes. J Magn Reson 2005;173:40–48. [PubMed: 15705511]
40. Gor'kov PL, Chekmenev EY, Fu RQ, Hu J, Cross TA. A large volume flat coil probe for oriented membrane proteins. J Magn, Reson 2006;181:9–20. [PubMed: 16580852]
41. Morris GA. Sensitivity enhancement in nitrogen-15 NMR: Polarization transfer using the INEPT pulse sequence. J Am Chem Soc 1980;102:428–429.
42. Neuhaus, D. Encyclopedia of Nuclear Magnetic Resonance. Grant, DM.; Harris, RK., editors. Wiley; Chichester: 1996. p. 3290
43. Hartmann SR, Hahn EL. Nuclear double resonance in the rotating frame. Phys Rev 1962;128:2042.
44. Metz G, Wu X, Smith SO. Ramped-amplitude cross polarization in magic-angle-spinning NMR. J Magn Reson Ser A 1994;110:219–227.
45. Warschawski DE, Devaux PF. Polarization transfer in lipid membranes. J Magn Reson 2000;145:367–372. [PubMed: 10910707]
46. Khitrin, AK.; Fung, BM.; McGeorge, G. Encyclopedia of Nuclear Magnetic Resonance. Grant, DM.; Harris, RK., editors. Wiley; Chichester: 2002. p. 91
47. Bennett AE, Rienstra CM, Auger M, Lakshmi KV, Griffin RG. Heteronuclear decoupling in rotating solids. J Chem Phys 1995;103:6951–6958.
48. Fung BM, Khitrin AK, Ermolaev K. An improved broadband decoupling sequence for liquid crystals and solids. J Magn Reson 2000;142:97–101. [PubMed: 10617439]
49. Shaka AJ, Keeler J, Freeman R. Evaluation of a new broadband decoupling sequence: WALTZ-16. J Magn Reson 1983;53:313–340.
50. Mohebbi A, Shaka AJ. Improvements in carbon-13 broadband homonuclear cross-polarization for 2D and 3D NMR. Chem Phys Lett 1991;178:374–378.
51. Dvinskikh SV, Sitnikov R, Furó I. $^{13}$C PGSE NMR experiment with heteronuclear dipolar decoupling to measure diffusion in liquid crystals and solids. J Magn Reson 2000;142:102–110. [PubMed: 10617440]
52. Sinha N, Grant CV, Wu CH, De Angelis AA, Howell SC, Opella SJ. SPINAL modulated decoupling in high field double- and triple-resonance solid-state NMR experiments on stationary samples. J Magn Reson 2005;177:197–202. [PubMed: 16137902]
53. Rothgeb TM, Oldfield EJ. Nitrogen-14 nuclear magnetic resonance spectroscopy as a probe of lipid bilayer headgroup structure. J Biol Chem 1981;256:6004–6009. [PubMed: 6894596]
54. Santos JS, Lee DK, Ramamoorthy A. Effects of antidepressants on the conformation of phospholipid headgroups studied by solid-state NMR. Magn Reson Chem 2004;42:105–114. [PubMed: 14745789]
55. Smith R, Separovic F, Bennett FC, Cornell BA. Melittin induced changes in lipid multilayers: a solid-state NMR study. Biophys J 1992;63:469–474. [PubMed: 1420892]
56. Seelig J, Macdonald PM, Scherer PG. Phospholipid headgroups as sensors of electric charge in membranes. Biochemistry 1987;26:7535–7541. [PubMed: 3322401]
57. Semchyschyn DJ, Macdonald PM. Conformational response of the phosphatidylcholine headgroup to bilayer surface charge: torsion angle constraints from dipolar and quadrupolar couplings in bicelles. Magn Reson Chem 2004;42:89–104. [PubMed: 14745788]
58. Prosser RS, Bryant H, Bryant RG, Vold RR. Lanthanide chelates as bilayer alignment tools in NMR studies of membrane-associated peptides. J Magn Reson 1999;141:256–260. [PubMed: 10579948]
59. Ramamoorthy A, Thennarasu S, Lee DK, Tan A, Maloy L. Solid-state NMR investigation of the membrane-disrupting mechanism of antimicrobial peptides MSI-78 and MSI-594 derived from Magainin 2 and Melittin. Biophys J 2006;91:206–216. [PubMed: 16603496]
60. Lindstrom F, Williamson PTF, Grobner G. Molecular insight into the electrostatic membrane surface potential by N-14/P-31 MAS NMR spectroscopy: Nociceptin-lipid association. J Am Chem Soc 2005;127:6610–6616. [PubMed: 15869282]

61. Lindstrom F, Bokvist M, Sparrman T, Grobner G. Association of amyloid-beta peptide with membrane surfaces monitored by solid state NMR. Phys Chem Chem Phys 2002;4:5524–5530.

62. Ramamoorthy A, Thennarasu S, Tan A, Gottipati K, Sreekumar S, Heyl DL, An FYP, Shelburne CE. Deletion of all cycteines in Tachyplesin I abolishes hemolytic activity and retains antimicrobial activity and LPS selective binding. Biochemistry 2006;45:6529–6540. [PubMed: 16700563]

63. Lu JX, Damodaran K, Lorigan GA. Probing membrane topology by high-resolution H-1-C-13 heteronuclear dipolar solid-state NMR spectroscopy. J Magn Reson 2006;178:283–287. [PubMed: 16275029]

64. Dvinskikh S, Dürr U, Yamamoto K, Ramamoorthy A. A high resolution solid state NMR approach for the structural studies of bicelles. J Am Chem Soc 2006;128:6326. [PubMed: 16683791]

65. Park SH, Prytulla S, De Angelis AA, Brown JM, Kiefer H, Opella SJ. High-resolution NMR spectroscopy of a GPCR in aligned bicelles. J Am Chem Soc 2006;128:7402–7403. [PubMed: 16756269]

66. Prosser RS, Hunt SA, DiNatale JA, Vold RR. Magnetically aligned membrane model systems with positive order parameter: Switching the sign of $S_{zz}$ with paramagnetic ions. J Am Chem Soc 1996;118:269–270.

67. Prosser RS, Hwang JS, Vold RR. Magnetically aligned phospholipid bilayers with positive ordering: A new model membrane system. Biophys J 1998;74:2405–2418. [PubMed: 9591667]

68. Sternin E, Bloom M, Mackay AL. De-Pakeing of NMR spectra. J Magn Reson 1983;55:274–282.

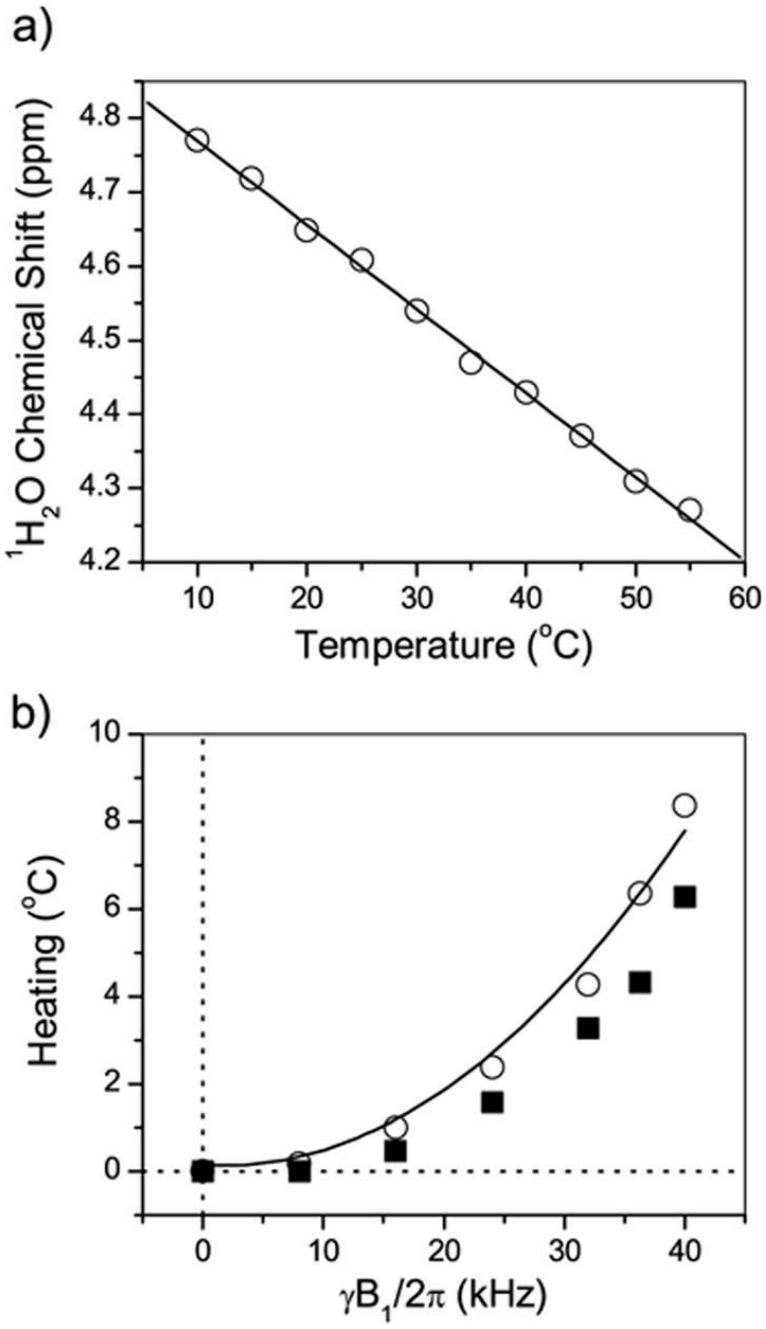


**Figure 1.**

(a) Variation of the chemical shift of water protons in a bicelle sample with the temperature. The proton chemical shift of water was set at 4.6 ppm at 25°C. (b) Open symbols represent the heating effect versus the RF field strength. The line is the fit to a second power dependence. Solid symbols represent the temperature gradient in the sample volume induced by the RF irradiation.

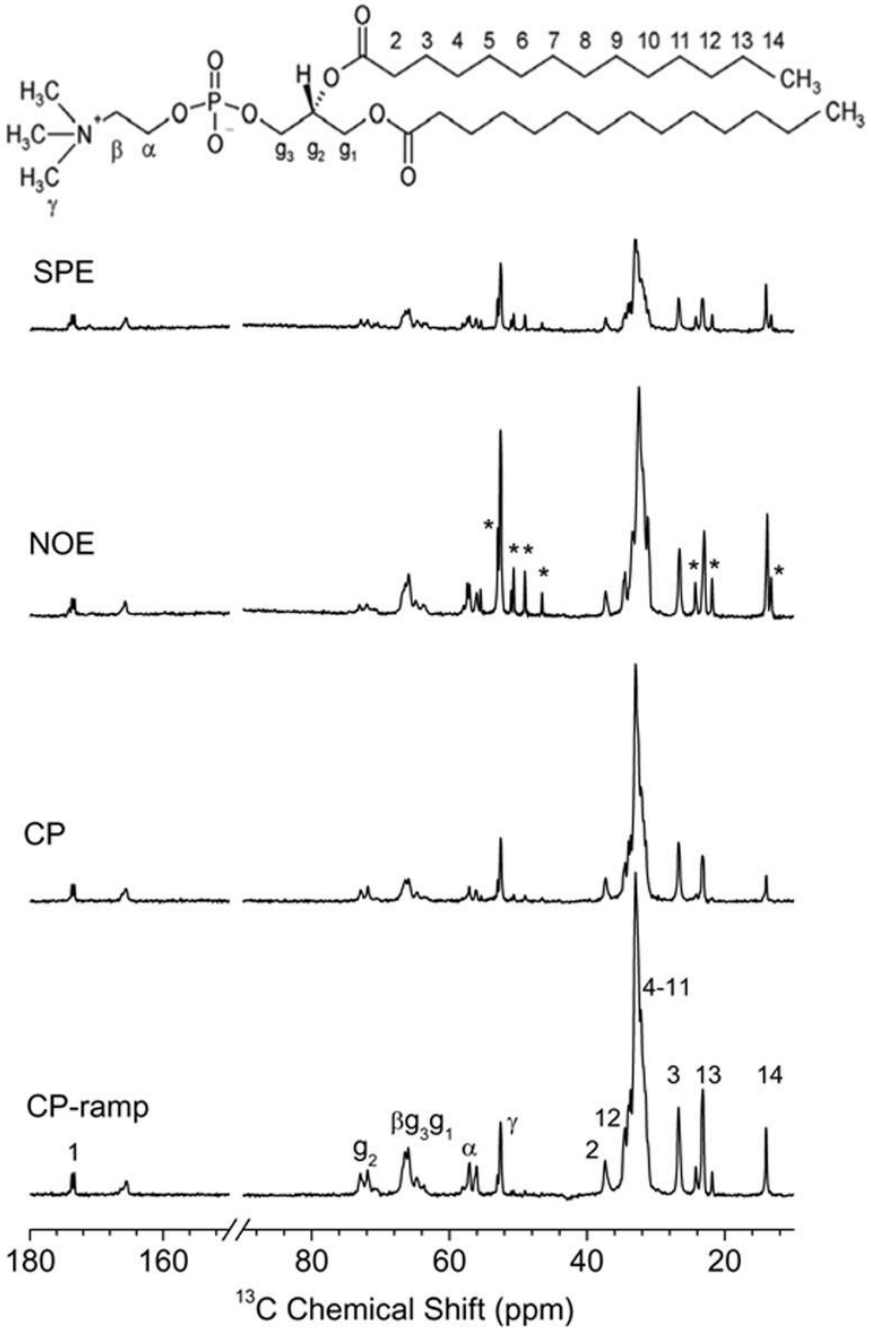


**Figure 2.**

Comparison of the $^{13}$C spectra of DMPC/DHPC bicelles at 37°C measured with different sensitivity enhancement techniques: (a) 90° single pulse excitation (SPE), (b) NOE, (c) constant amplitude CP, and (d) ramped amplitude CP. Signals from DHPC detergent, observed most clearly in NOE and SPE spectra, are indicated by asterisks. The molecular structure of DMPC is shown at the top.

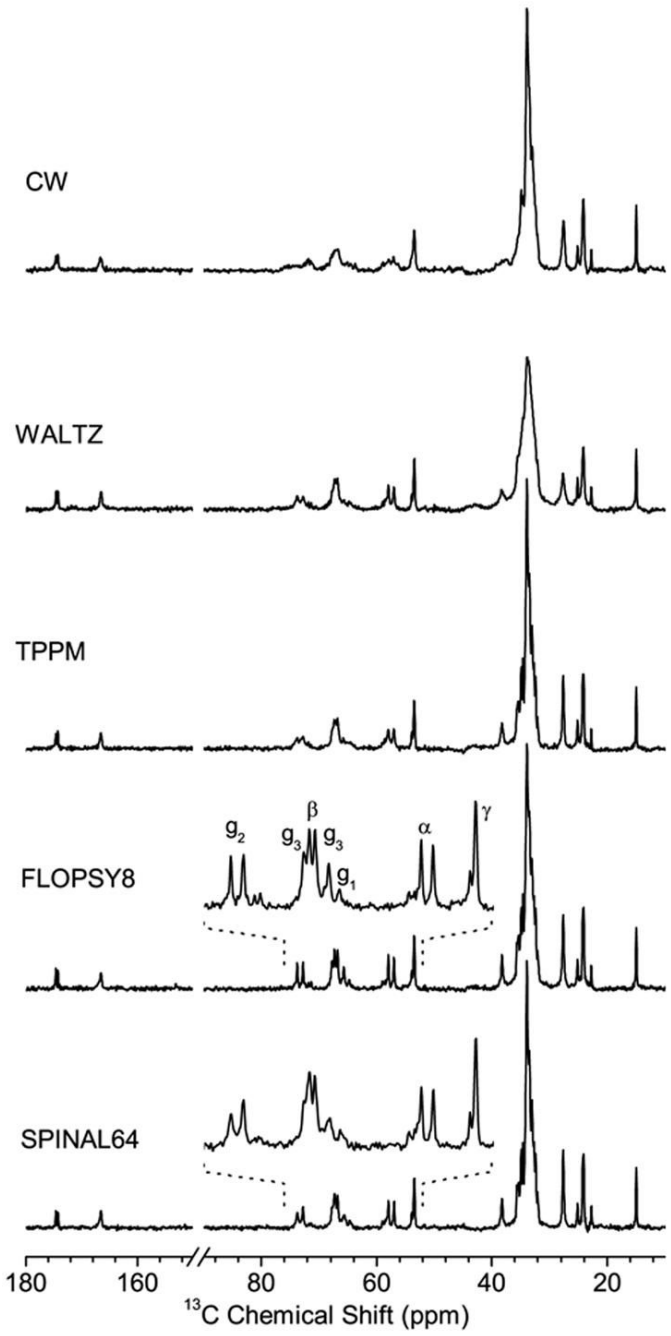


**Figure 3.**
$^{13}$C spectra of DMPC/DHPC bicelles at 37°C measured with different heteronuclear decoupling sequences. The proton decoupler RF field strength was set at 20 kHz. The RF decoupler frequency was set to a value that resulted in an optimal resolution for the crowded chain-carbon region when CW irradiation was used. The pulse durations were optimized for WALTZ-16 and FLOPSY-8 sequences, while both pulse durations and RF phase shifts were optimized for TPPM and SPINAL-64 schemes. The spectral region containing signals from the lipid head group and glycerol sites is expanded for an easy comparison of spectra obtained using the FLOPSY and SPINAL decoupling sequences.

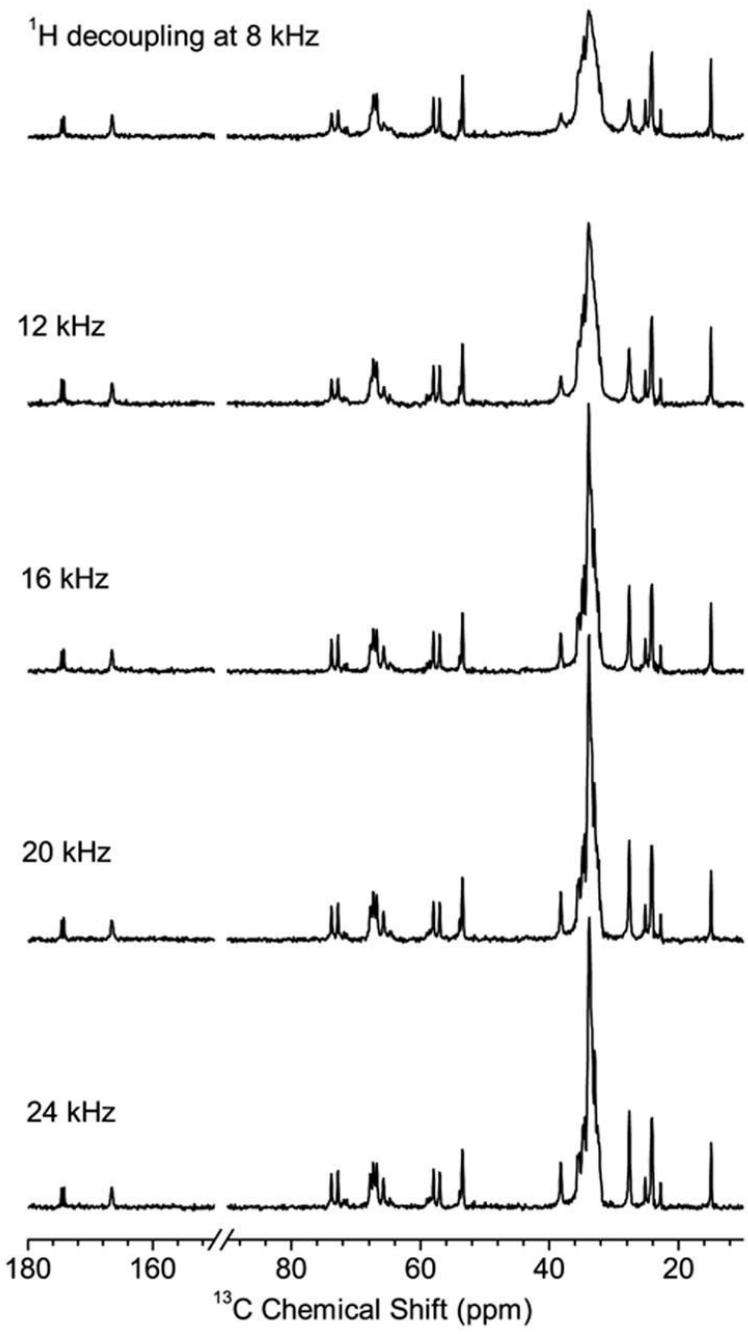


**Figure 4.**
$^{13}$C spectra of DMPC/DHPC bicelles at 37°C obtained using the FLOPSY-8 proton decoupling sequence at different decoupling power levels.

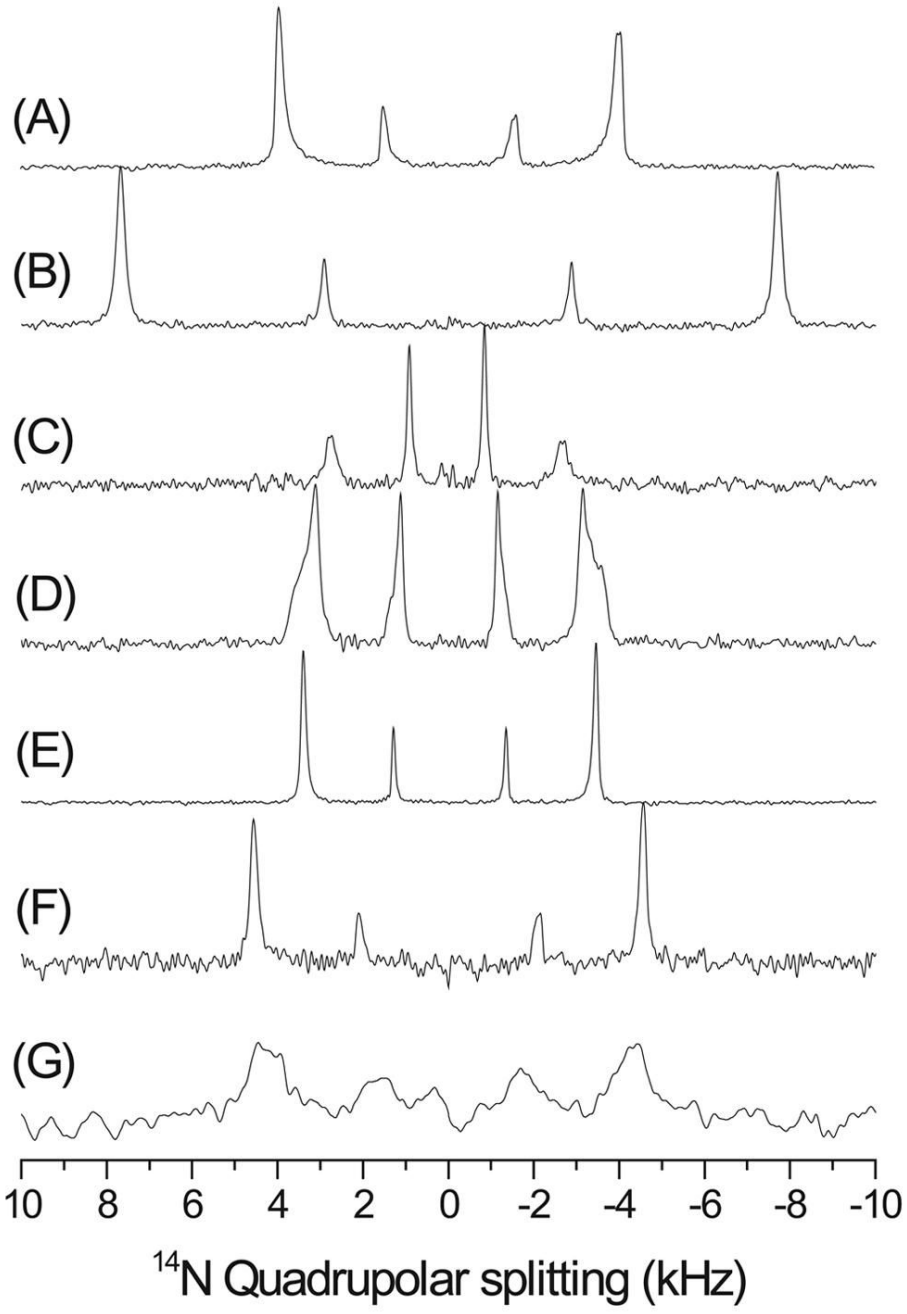


**Figure 5.**
$^{14}$N quadrupole coupling spectra of magnetically aligned DMPC:DHPC bicelles, q=3.5, showing the influence of admixing different substances: (A) Pure DMPC:DHPC bicelles; (B) in the presence of of $Yb^{3+}$ ions, resulting in 'flipped' bicelles; (C) 2.0 mole % desipramine; (D) 2.0 mole % MSI-78; (E) 0.5 mole % MSI-78; (F) 20.0 mole % negatively charged lipid DMPG in the presence and (G) absence of 150 mM NaCl.